Method of Setting Nozzle Intervals at the Finishing Scale Breaker

Sung Cho Kim, Jong Wook Choi*
School of Mechanical and Automotive Engineering, Sunchon National University, Suncheon-City, Chonnam 540-742, Korea
Jin Won Choi
Technical Research Laboratories, POSCO, Gwangyang-City, Chonnam 545-090, Korea

The scale is removed from the strip by high pressure hydraulic descaling at the FSB(Finishing Scale Breaker). Recently, the spray height of nozzle has a trend to be shorter for the purpose of increasing the impact pressure by the high pressure water jet. Here, the nozzle intervals should be decided after considering the impact pressure and the temperature distribution on the strip. In other words, the minimum of impact pressure at the overlap of spray influences the surface grade of the strip due to scale and the overlap distance of the spray affects the temperature variation in the direction of the width of strip. In the present study, the impact pressure of the high pressure water jet is measured by the hydraulic descaling system and calculated with regard to the lead angle of 15° and the offset angle of 15°, and then the temperature distribution and the temperature variation are calculated at the overlap distances of 0 mm, 10 mm, 20 mm, and 30 mm, respectively. The method of setting nozzle intervals is shown by utilizing these results.

Key Words : FSB(Finishing Scale Breaker), Impact Pressure, Temperature Distribution, Overlap Distance, Temperature Variation

Nomenclature

c : Specific heat (J/kg℃)
H : Vertical distance of spray (mm)
h : Convective heat transfer coefficient (W/m²℃)
IP : Impact pressure (bar)
k : Thermal conductivity of strip (W/m℃)
k_{water} : Thermal conductivity of water (W/m℃)
L : Characteristic length of the sensor of impact pressure (m)
Nu : Nusselt number (hL/k_{water})
Re : Reynolds number (VL/υ_{water})
T : Temperature (℃)
t : Time (sec)
V : Velocity of the high pressure water jet (m/s)

Greek Symbols

α : Thermal diffusivity (m²/s)
θ_l : Lead angle (°)
θ_o : Offset angle (°)
θ_s : Spray angle (°)
υ_{water} : Kinematic viscosity of water (m²/s)
ρ : Density(kg/m³)

* Corresponding Author,
E-mail : choijw99@postown.net
TEL : +82-61-750-3957; **FAX** : +82-61-753-3962
School of Mechanical and Automotive Engineering, Sunchon National University, Suncheon-City, Chonnam 540-742, Korea. (Manuscript **Received** May 15, 2002; **Revised** August 7, 2003)

1. Introduction

The scale on the strip is removed by high pressure water jet at the FSB(Finishing Scale Breaker). The nozzles for the high pressure water jet are located at the header with the lead angle and the offset angle. The function of the lead angle is to prevent the scale from entering the FM (Finishing Mill), and the nozzles are installed at the lead angle of 15° conventionally. The impact pressure is still about 97% of the maximum value at the lead angle of 15°(Marston, 1995). The function of the offset angle is to prevent the high pressure water jets from overlapping each other. If

the high pressure water jets overlap each other without the offset angle, the impact pressure will be decreased at the overlap. Therefore, the nozzles maintain the offset angle of 15° in general.

Recently, the spray height of nozzle has a trend to be shorter and shorter for the purpose of increasing the impact pressure by the high pressure water jet. Here the nozzle intervals should be decided after considering the impact pressure and the temperature distribution on the strip. However, there is a few literatures related to it. In general, the overlap distance for the spray width is 25-30 mm, when the spray height of nozzle is 240-300 mm (Bagshaw and Kimpton, 1995).

The overlap distance affects the impact pressure acting on the strip and the temperature variation in the direction of the width of strip. That is, the minimum of impact pressure and the temperature in the direction of the width of strip vary according to the overlap distance of the spray width. If the overlap distance is increased, the minimum of impact pressure is increased and the scale on the strip is removed well. However, the temperature drop of the strip is increased owing to increasing the area under high pressure water jet. Therefore, we could not increase the impact pressure extremely, as the strip should be kept over A_3 transition temperature for the hot rolling. On the contrary, if the overlap distance is decreased, the temperature drop of the strip is decreased. However, the minimum of impact pressure is decreased, the scale on the overlaps of the strip is not removed well. Besides, the optimal design for the FSB needs the thermal analysis in the strip because the quality of the rolled steel product is depended on the temperature distribution of the strip in the rolling process. In other words, the overlap distance should be decided after consideration of the minimum of impact pressure, the temperature drop of the strip, and the temperature variation in the direction of the width of strip.

In the present study, the distribution of impact pressure is measured at the lead angle of 0° and the offset angle of 0° using the descaling simulator, and the distribution of impact pressure is calculated at the lead angle of 15° and the offset angle of 15° according to the overlap distances of 0 mm, 10 mm, 20 mm, and 30 mm, respectively. These angles are the operating conditions at the FSB in general.

The convective heat transfer coefficient is necessary to the analysis of temperature distribution. The convective heat transfer coefficient used in the calculation is obtained from the equation as a function of the impact pressure (Choi and Choi, 2002) and then the temperature distribution in the strip is calculated by the FDM(Finite Difference Method). Finally, the reasonable overlap distance for the spray width is decided by utilizing these results.

2. The Distribution of Impact Pressure

2.1 The experiment on the impact pressure

The impact pressure of high pressure water jet is measured by the descaling simulator as shown in Fig. 1. This apparatus was manufactured for measuring the temperature variation and for observing the scale on the specimen during the process of the hydraulic descaling originally. The descaling simulator consists of the carriage(1), the specimen(2), the step motor(3), the nozzle header(4), the air cylinder(5), the spray nozzle (6), another air cylinder(7) as shown in Fig. 1. The lead angle and the spray height are controlled by the air cylinder(5) and (7), respectively.

For measuring the impact pressure, a pressure sensor instead of the specimen(2) is laid on the carriage as shown in Fig. 2. The sensor of impact

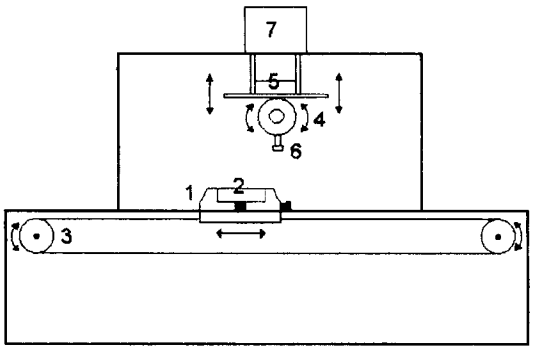

Fig. 1 The schematic diagram of the descaling simulator

pressure used in the present experiment is the type of load cell. The area of sensing the impact force is 0.5 cm^2. The impact force in the direction of the spray width is measured by moving a carriage at 5 mm/s. The data of impact force is obtained at 0.5 mm intervals in the direction of the spray width. Impact force divided by the area of sensor gives the impact pressure.

2.2 The results of the experiment on the impact pressure

The distribution of impact pressure at the spray pressure of 200 bar and the spray height of 140 mm is shown in Fig. 3. The average impact pressure is approximately 7 bar. The distribution of impact pressure has nearly a symmetric pattern and the impact pressures on the both sides are higher than those at the center.

The spray nozzle (DNR type) used in the experiment has the spray angle of 28° and the orifice diameter of 3.4 mm at the minor axis and 4.5 mm at the major axis, respectively. The water flow rate is 118 liter/min at the spray pressure of 150 bar. These values were given by nozzle maker.

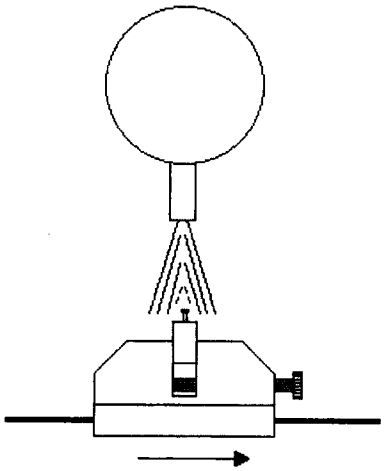

Fig. 2 The schematic diagram of measuring instrument for the impact pressure

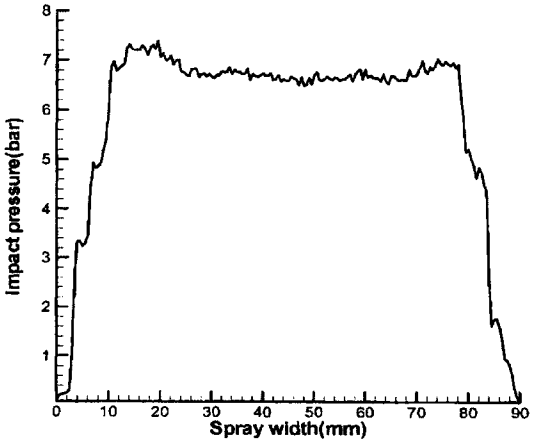

Fig. 3 The distribution of impact pressure in the direction of the spray width (P=200 bar, H=140 mm)

2.3 The distribution of impact pressure with regard to the lead angle and the offset angle

The distribution of impact pressure with regard to the lead angle and the offset angle could not be obtained from the experiment using the descaling

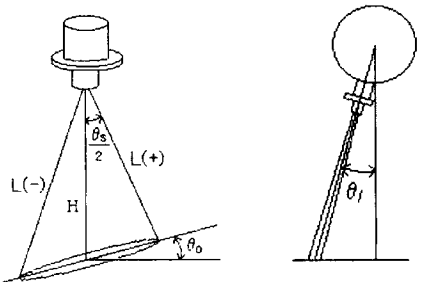

Fig. 4 The lead angle and the offset angle of the spray nozzle

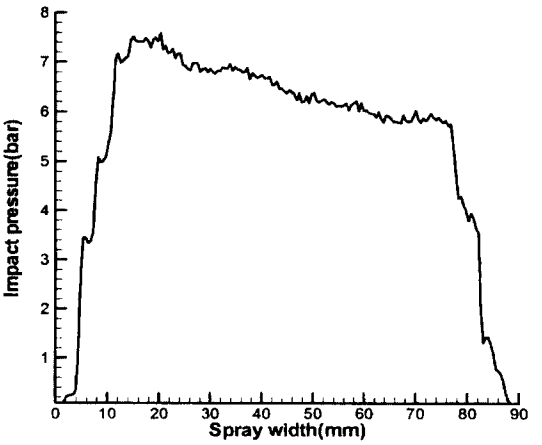

Fig. 5 The distribution of the impact pressure at lead angle of 15° and offset angle of 15°

simulator. In the present study, the distribution of impact pressure with regard to these angles is obtained. Here, the spray distance is defined as the length from the nozzle tip to the strip.

The spray distance may be increased or decreased by the lead angle and the offset angle as shown in Fig. 4. When the spray distances are increased or decreased, these values are obtained from Eq. (1) and Eq. (2), respectively, and these equations are satisfied in the range of $0° \leq \theta_s/2 + \theta_l < 90°$.

$$L(+) = \frac{H \tan(\theta_s/2) \sin \theta_l \sin \theta_o}{\cos(\theta_s/2 + \theta_l \sin \theta_o)} \quad (1)$$

$$L(-) = \frac{H \tan(\theta_s/2) \sin \theta_l \sin \theta_o}{\cos[(90° - \theta_s/2) - (90° - \theta_l) \sin \theta_o]} \quad (2)$$

The distribution of impact pressure is calculated by Eq. (1) and Eq. (2) at the lead angle of 15° and the offset angle of 15° as shown in Fig. 5. The spray distances get shorter in the left side of the spray center point and become longer in the right

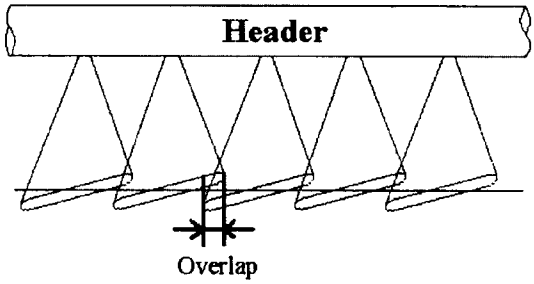

Fig. 6 The overlap distance at the FSB

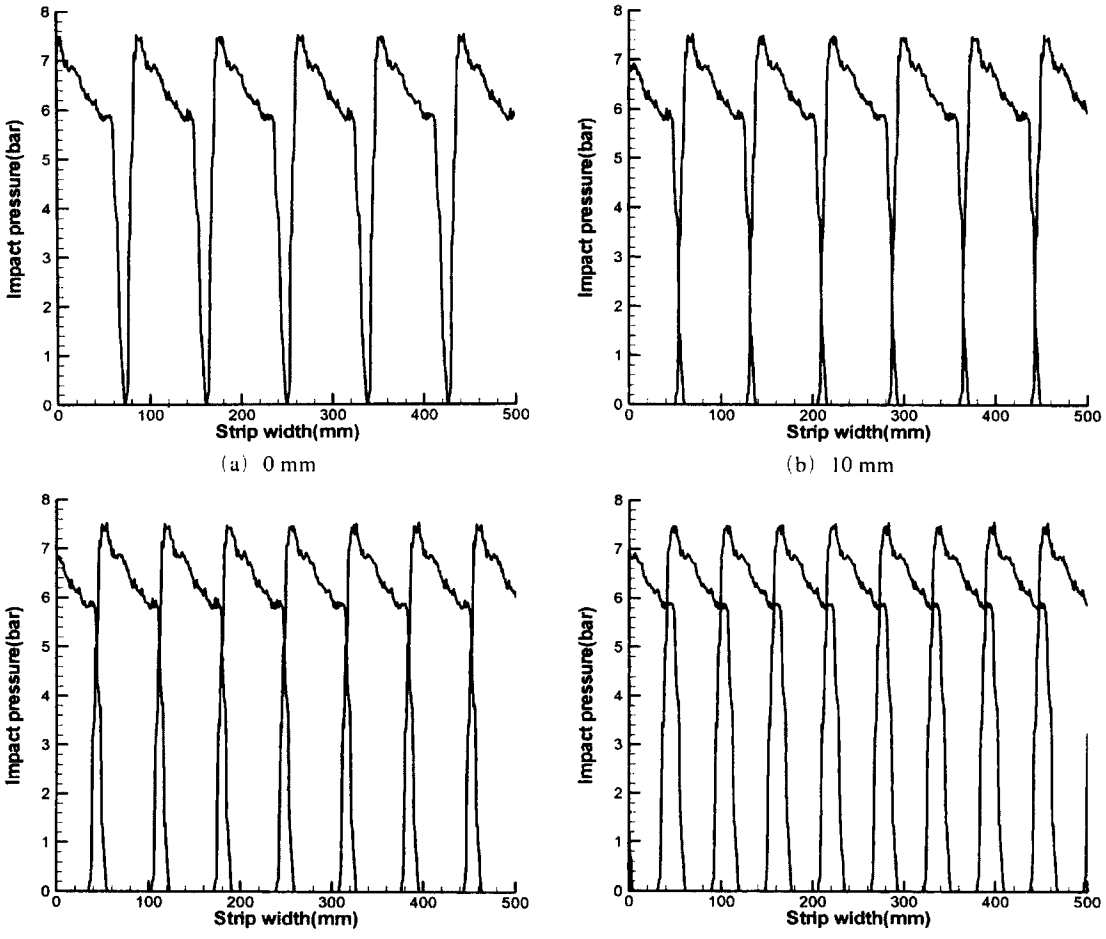

(a) 0 mm (b) 10 mm

(c) 20 mm (d) 30 mm

Fig. 7 The distribution of the impact pressure with overlap

side of the spray center point owing to the lead angle and the offset angle. On this account, the impact pressures are increased and decreased at the left side, and the right side respectively.

The spray nozzles are arranged in a row at the FSB header and the spray patterns are overlapped as shown in Fig. 6. In the present study, the distributions of impact pressure are calculated at the overlap distances of 0 mm, 10 mm, 20 mm, and 30 mm, respectively. The distribution of impact pressure is shown in Fig. 7(a) at the overlap distance of 0 mm. These values are calculated at the range of the strip width of 500 mm only, owing to the symmetric patterns in the direction of the width of strip. The scale should not be removed well at the overlap distance of 0 mm, because the impact pressures are approximately 0 bar at the both ends of spray. The distributions of impact pressure are shown in Fig. 7(b)-(d) at the overlap distance of 10 mm, 20 mm, and 30 mm respectively, and the minimums of impact pressure are approximately 3.5 bar, 5.8 bar and 6 bar respectively. If the minimums of impact pressure are increased at the overlap, the scale will be removed well. However, as the temperature drop is increased at the overlap, the temperature variation will also be increased in the direction of the width of strip. In this account, the overlap distance should be determined with regard to both the impact pressure and the temperature variation.

3. The Temperature Distribution

3.1 The convective heat transfer coefficient

The convective heat transfer coefficient is necessary to the analysis of temperature distribution. In general, the convective heat transfer coefficient varies with the velocity of the fluid, the type of flow, the geometry of the body, the flow passage area, the physical properties of the fluid, and so on. The convective heat transfer coefficient is increased according to the increasing spray pressure and the decreasing spray height, because the velocity of water jet is increased on the strip. Therefore, the convective heat transfer coefficient can be correlated with the spray pressure and the spray height. Also, the spray pressure and the spray height are correlated with the impact pressure on the strip, and two independent variables (the spray pressure and the spray height) can be reduced to one independent variable (the impact pressure). The convective heat transfer coefficient can be obtained from comparing the calculated temperature with the experimental temperature as shown in Fig. 8. The convective heat transfer coefficients with the impact pressure can be represented by non-dimensional variables such as the Nusselt number and Reynolds number as

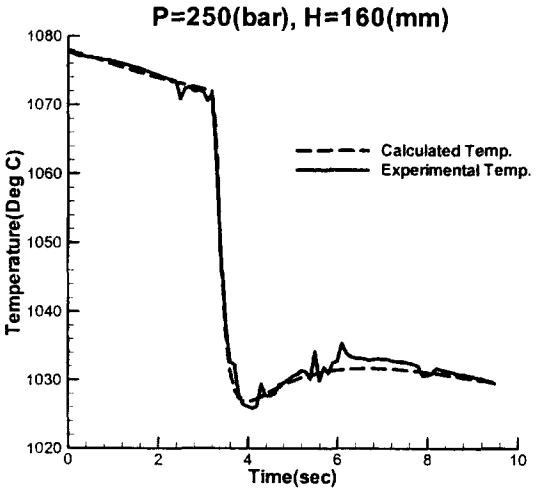

Fig. 8 The temperature variation at IP=6.94 (bar)

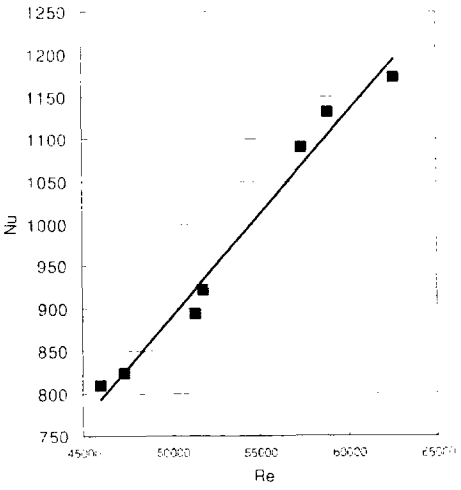

Fig. 9 The variation of Nusselt number with Reynolds number

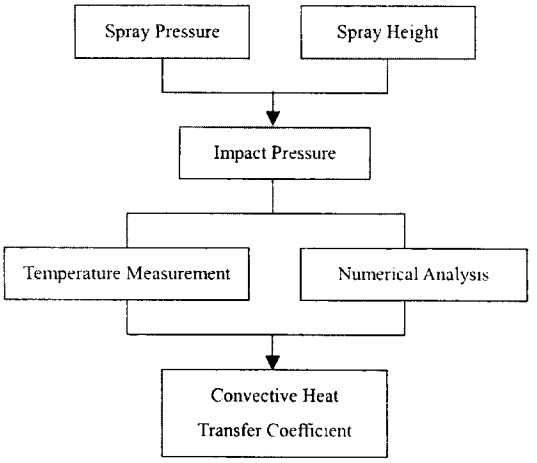

Fig. 10 The flow chart for calculating the convective heat transfer coefficient

shown in Fig. 9. Equation (3) is obtained from these results.

$$Nu=0.0241\times \mathrm{Re}-314.67 \tag{3}$$

These processes for obtaining the convective heat transfer coefficient are shown as the flow chart in Fig. 10 (Choi and Choi, 2002). The convective heat transfer coefficients in the direction of the width of strip are obtained from the distributions of impact pressure as shown in Fig. 7 and are similar in patterns to the result of impact pressures. The convective heat transfer coefficients by the air and the residual water used in the analysis of temperature distribution are 120 W/m^2℃ (Nu=0.34) and 185 W/m^2℃ (Nu=0.52), respectively.

3.2 The analysis of temperature distribution

The temperature distribution of the strip through the high pressure water jet is analyzed assuming that the temperature variation in the direction of the length of strip is ignored and the effect of the scale is also disregarded. That is, the temperature distribution of the strip is analyzed at the two dimensional section of it. Two dimensional, time dependent heat conduction equation (Özisik, 1985) is expressed by Eq. (4).

$$\frac{\partial T}{\partial t}=\alpha\left[\frac{\partial^2 T}{\partial x^2}+\frac{\partial^2 T}{\partial y^2}\right] \tag{4}$$

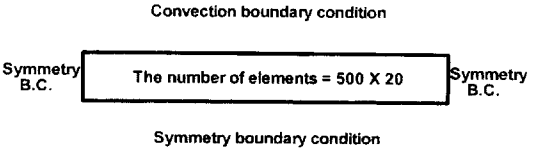

Fig. 11 The boundary conditions in calculated domain

Where α is $k/\rho c$, and the thermal conductivity (k), the density (ρ) and the specific heat (c) of the strip are 27.6 W/m℃, 7,870 kg/m^3, and 875 J/kg℃, respectively. Therefore, the thermal diffusivity (α) used in the calculation is 4.008×10^{-6} m^2/s.

Equation (4) is solved by the explicit finite difference equation using forward differencing for the time derivative and central differencing for the space derivative. The boundary conditions on the computational domain consist of the convection boundary and the symmetry boundary as shown in Fig. 11. Here, both of the temperatures of air and water are 30℃, and the initial temperature of the strip is 1100℃. The dimensions of the strip used in the calculation are 500 mm(Width)×20 mm(Thickness). The number of the grid elements is 10,000(500×20) and the grid step is 0.001 m in size and time step is 0.002 sec. The values satisfy the stability condition (Anderson et al., 1984).

The temperature distributions are calculated by three steps. These steps are consist of the heat transfer before the hydraulic descaling(0 sec−3.7 sec), the heat transfer during the hydraulic descaling(3.7 sec−3.7006 sec), and the heat transfer after the hydraulic descaling(3.7006 sec−10 sec). The spraying time of 0.0006 sec obtained from the spray thickness of 6 mm divided by the velocity of moving strip of 60 mpm. Here, the value of spray thickness is obtained from the spray pattern observed on the lead plate.

3.3 The results of temperature distribution

The temperature distributions are shown in Fig. 12 at the overlap of 0 mm, 10 mm, 20 mm, and 30 mm, respectively. These results are calculated at 6.3 sec after the hydraulic descaling is finished(namely at 10 sec). That means the time required between the hydraulic descaling and the

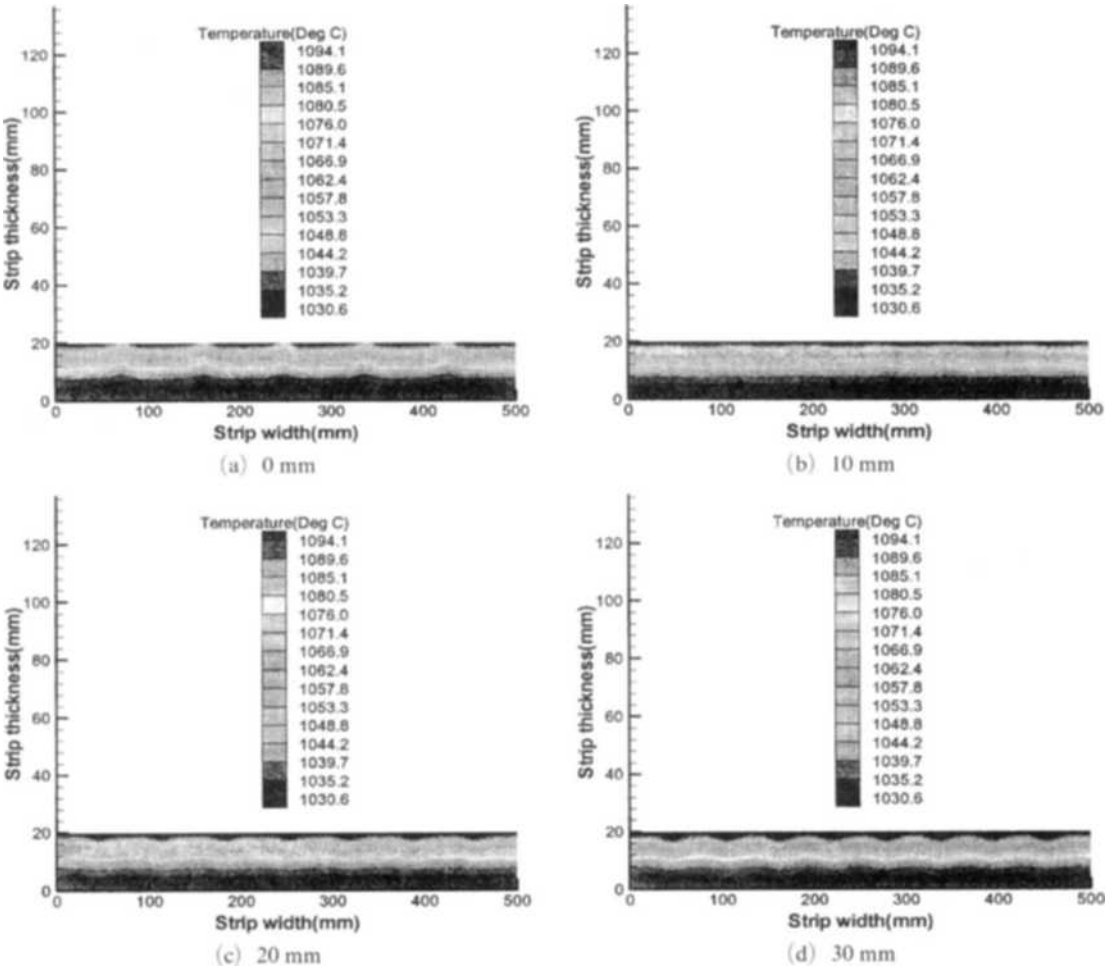

Fig. 12 The temperature distribution with overlap

hot rolling in the rolling mill. The temperature variation in the direction of the width of strip at the overlap of 10 mm is lower than those for other cases as shown in Fig. 12(b). In case of the overlap distance of 0 mm, the temperature variation is higher than that at the overlap of 10 mm owing to the insufficient water jet at the overlap as shown in Fig. 12(a), and in cases of the overlap distance of 20 mm and 30 mm, the temperature variations are higher than that at the overlap of 10 mm owing to the excessive water jet at overlap as shown in Fig. 12(c)-(d).

3.4 The results of temperature variation with time

The temperature variations with respect to time are calculated at overlap of 0 mm, 10 mm, 20 mm, and 30 mm as shown in Fig. 13, respectively. The solid lines represent the temperature variation at the maximum of temperature drop of the strip surface. The dotted lines represent the temperature variation at the minimum of temperature drop of the strip surface. The temperatures are dropped steeply during the hydraulic descaling process and restored after the hydraulic descaling process. In the case of overlap of 0 mm, the minimum of temperature drop occurs at the overlap owing to the lower flow rate. Therefore, the difference of the temperature drops is larger than those in the cases of overlaps of 10 mm, 20 mm, and 30 mm during the descaling process as shown in Fig. 13(a). In case of overlap of 10 mm, the

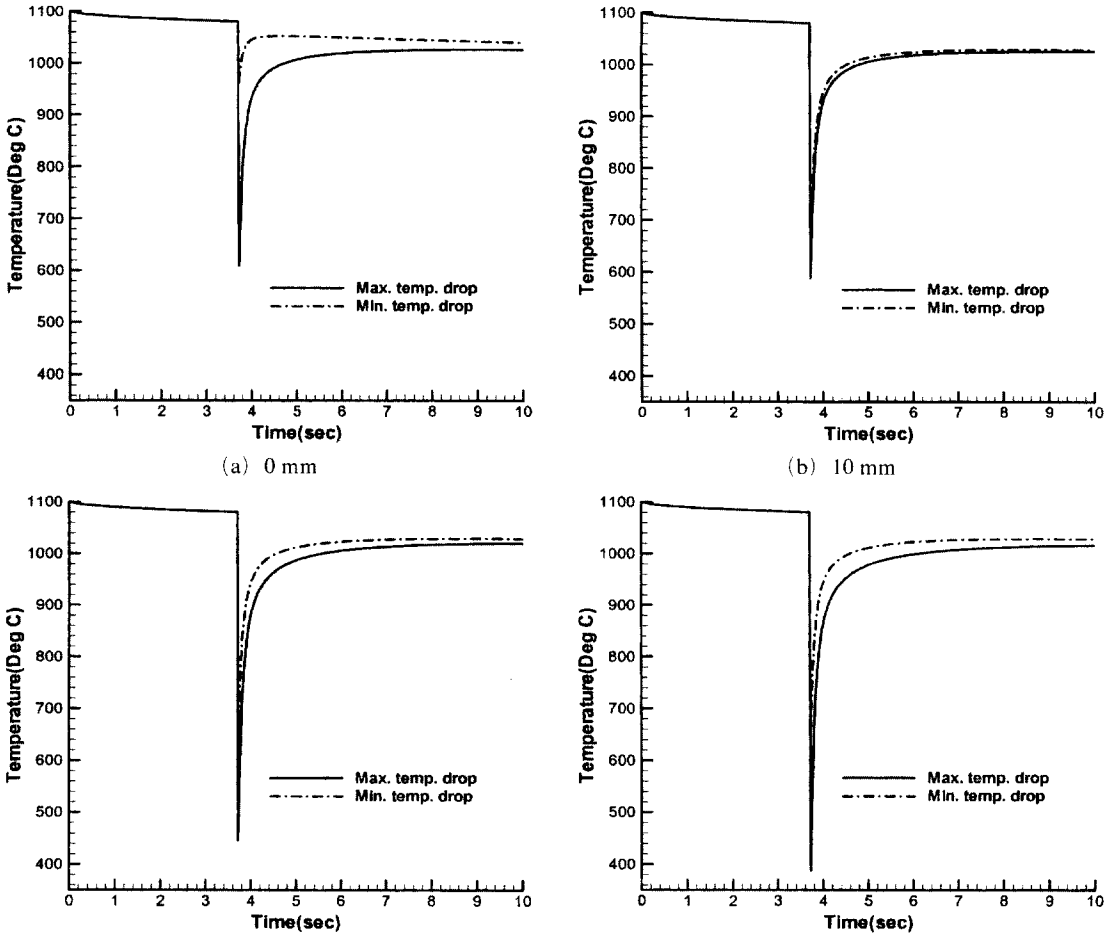

Fig. 13 The temperature variation with overlap

difference of temperature drop is less than the case of 0 mm as shown in Fig. 13(b). In the cases of overlap of 20 mm and 30 mm, the differences of temperature drops are large during the descaling process, however, the differences are narrowed with respect to time as shown in Fig. 13(c)-(d), and the values are larger than that at the overlap of 10 mm.

4. Conclusion

In the present study, the distribution of impact pressure was measured at the lead angle of 0° and the offset angle of 0° using the descaling simulator, and the distribution of impact pressure was calculated at the lead angle of 15° and the offset angle of 15° by the Eq. (1) and Eq. (2). As a result, the minimums of impact pressure were 0 bar, 3.5 bar, 5.8 bar, and 6.0 bar according to the overlap distances of 0 mm, 10 mm, 20 mm, and 30 mm, respectively. In the cases of the overlap of 20 mm and 30 mm, the difference of the impact pressure was only about 0.2 bar in spite of the difference of 10 mm in the overlap distance. As the flow rate at the overlap of 30 mm is higher than that at the overlap of 20 mm, the temperature drop at the overlap of 30 mm is larger than that at the overlap of 20 mm though the minimum of impact pressure at these overlap is alike.

The convective heat transfer coefficient used in the calculation was obtained from comparing the calculated temperature with the experimental tem-

perature and then the temperature distribution in the strip was calculated by FDM. As a result, the temperature variation at the overlap of 10 mm was smaller than those at the overlap of 0 mm, 20 mm, and 30 mm.

As a result, if only the minimum of impact pressure is considered, the overlap distance of 20 mm is most suitable. If only the temperature variation is considered, the overlap distance of 10 mm is most suitable. In general, the overlap distance have been set up as 10~15% of the spray width. The overlap distance of 10 mm is the value of about 11% for the spray width of 90 mm. On the other hand, the basic method of setting nozzle intervals was shown in the present study. In the further study, the distributions of the impact pressure and the temperature will be obtained from 3-dimensional flow analysis in overlap sections, and then the nozzle intervals obtained from the overlap distances will be applied to a rolling mill.

Acknowledgment

This work was supported in part by Research Foundation of Engineering College, Sunchon National University and partially by the Brain Korea 21 Project. The authors would like to thank for these supports.

References

Anderson, D. A., Trannehill, J. C. and Pletcher, R. H., 1984, *Computational Fluid Mechanics and Heat Transfer*, Hemisphere Publishing Corporation, NewYork, p. 108.

Bagshaw, P. and Kimpton, R., 1995, "Optimisation of the Hydraulic Descaling System at the BHP New Zealand Steel Hot Strip Mill," *Proceeding of 1st International Conference on Hydraulic Descaling in Rolling Mills*, Painters Hall, London.

Choi, J. W. and Choi, J. W., 2002, "Convective Heat Transfer Coefficient for High Pressure Water Jet," *ISIJ International*, Vol. 42, No. 3, pp. 283~289.

Marston, H. F., 1995, "Influence of Scale Structure on the Effectiveness of Descaling," *Proceeding of 1st International Conference on Hydraulic Descaling in Rolling Mills*, Painters Hall, London.

Özişik, M. N., 1985, *Heat Transfer*, McGraw-Hill, New York, p. 6.